

Tunable Charge Transport in Soluble Organic–Inorganic Hybrid Semiconductors

Yukari Takahashi, Rena Obara,[†] Kohei Nakagawa,[‡] Masayuki Nakano,[§] Jun-ya Tokita,[¶] and Tamotsu Inabe*

Division of Chemistry, Graduate School of Science, Hokkaido University, Sapporo 060-0810, Japan

Received August 24, 2007. Revised Manuscript Received October 12, 2007

The organic–inorganic hybrid tin iodide perovskites, A_2SnI_4 (A = organic ammonium), consist of inorganic layers bearing electronic functionality and organic layers that act as a template for the structure and are also able to tune the band structure. These hybrids are soluble in a wide range of solvents. Charge-transport measurements performed on single crystals indicate that the conductivity is high, despite band gaps of more than 1 eV, and strongly influenced by the type of cationic species A . The high conductivity is assumed to be due to spontaneous p-type doping in the as-grown crystals. The conductivity can be further enhanced by artificial hole doping. Since these materials can be processed in solution and display electronic performance comparable to conventional inorganic semiconductors, they show promise as a new class of tunable semiconductors of future technological importance.

Introduction

Many divalent metal ions (M^{II}) form layered perovskites, $A_2M^{II}X_4$, with halides (X). When A is an organic ammonium cation, two-dimensional inorganic layers completely separated by organic layers are formed. The organic layers are electronically inert but act as a template for the inorganic framework.^{1,2} Organic–inorganic hybrid transition-metal halides are generally good insulators (wide-gap semiconductors), but when M is a group 14 metal (Ge, Sn, Pb), they are semiconductors with narrower band gaps. In addition, a series of compounds with composition $A_2(CH_3NH_3)_{n-1}M_nI_{3n+1}$ can be obtained by varying the number of perovskite layers (n). These materials first attracted attention in the 1990s. For the $M = Pb$ system, studies have since been conducted in order to determine the correlation between the number of perovskite layers and the electronic structure^{3–5} as well as the dependence of the structure and optical properties on the type of organic species.^{6–8} Tin iodide compounds have a narrower band gap than those containing

Pb,^{4,9} and the parent cubic perovskite with composition $(CH_3NH_3)SnI_3$ ($n = \infty$) has been reported to exhibit metallic transport behavior.¹⁰ The dependence of the electrical conductivity on the number of perovskite layers has also been studied and was found to decrease as n decreases.¹¹ Surprisingly, although the tin iodide system is very attractive with respect to electrical properties, the transport properties of these compounds in single-crystal form have not been studied quantitatively. There is one report of conductivity measurements on single crystals of $(C_6H_5CH_2CH_2NH_3)_2SnI_4$.¹² However, instead of presenting the absolute conductivity as a function of temperature, the authors normalized this quantity to its room-temperature value. The chemical instability (reactivity) of crystals in the tin iodide system poses problems for accurate transport measurements, and conductivity measurements have thus far been performed mainly on compressed pellets, with spring-activated pins directly contacting the sample.^{10,11,13}

Since transport should be anisotropic in these layered compounds, their intrinsic properties can be obtained only when measurements are performed on single crystals. Therefore, we initiated our work with the goal of making good electrical contacts with the crystal, and we have developed a technique that gives moderate contact resistance. This has subsequently enabled us to measure the electrical conductivity of A_2SnI_4 organic–inorganic hybrids ($n = 1$) containing various organic cations. Two important findings resulted from our study. First, the electrical conductivity within the inorganic layer is rather high, reaching values as

* To whom correspondence should be addressed. E-mail: inabe@sci.hokudai.ac.jp.

[†] Present address: Ricoh Software Inc., Hakuyo-cho, Kitami 090-0013, Japan.

[‡] Present address: Canon Inc., Inkjet Supply Material Development Center, Saiwai-ku, Kawasaki 212-8530, Japan.

[§] Present address: DOWA Semiconductor Akita Inc., 1 Sunada, Iijima, Akita 011-0911, Japan.

[¶] Present address: AsahiKASEI Chemicals Corporation, Nobeoka 882-0015, Japan.

- (1) Mitzi, D. B. *Prog. Inorg. Chem.* **1999**, *48*, 1.
- (2) Mitzi, D. B. *J. Chem. Soc., Dalton Trans.* **2001**, 1.
- (3) Papavassiliou, G. C. *Prog. Solid State Chem.* **1997**, *25*, 125.
- (4) Papavassiliou, G. C.; Koutselas, I. B. *Synth. Met.* **1995**, *71*, 1713.
- (5) Umebayashi, T.; Asai, K.; Kondo, T.; Nakao, A. *Phys. Rev. B* **2003**, *67*, 155405.
- (6) Ishihara, T.; Takahashi, J.; Goto, T. *Phys. Rev. B* **1990**, *42*, 11099.
- (7) Venkataraman, N. V.; Bhagyalakshmi, S.; Vasudevan, S.; Seshadri, R. *Phys. Chem. Chem. Phys.* **2002**, *4*, 4533.
- (8) Sourisseau, S.; Louvain, N.; Bi, W.; Mercier, N.; Rondeau, D.; Boucher, F.; Buzaré, J.-Y.; Legein, C. *Chem. Mater.* **2007**, *19*, 600.

(9) Mitzi, D. B. *Chem. Mater.* **1996**, *8*, 791.

(10) Mitzi, D. B.; Field, C. A.; Schlesinger, Z.; Laibowitz, R. B. *J. Solid State Chem.* **1995**, *114*, 159.

(11) Mitzi, D. B.; Field, C. A.; Harrison, W. T. A.; Guloy, A. M. *Nature* **1994**, *369*, 467.

(12) Papavassiliou, G. C.; Koutselas, I. B.; Terzis, A.; Whangbo, M.-H. *Solid State Commun.* **1994**, *91*, 695.

(13) Mitzi, D. B.; Wang, S.; Field, C. A.; Chess, C. A.; Guloy, A. M. *Science* **1995**, *267*, 1473.

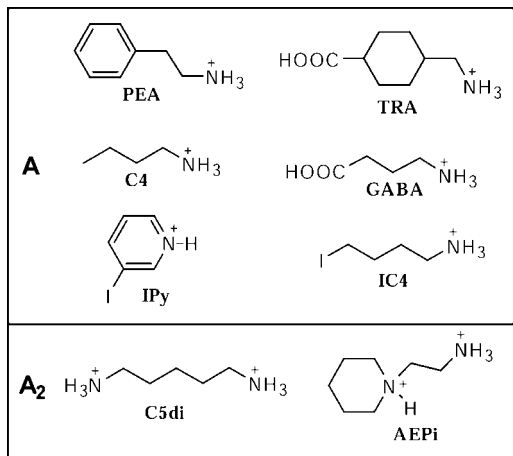


Figure 1. Organic cations used in the synthesis of A_2SnI_4 .

large as 0.1 S cm^{-1} at room temperature in as-grown crystals, and is also sensitive to the type of cationic species. Since the band gap always exceeds 1 eV in these compounds, such high conductivities are completely inconsistent with the electronic structure. Second, we found that the high conductivity results from low levels of spontaneous p-type doping and that the conductivity can also be increased by artificial hole doping. We present detailed charge-transport properties of single crystals of A_2SnI_4 , which have thus far proved difficult to measure, and show that the transport properties are tunable over a wide range.

Experimental Section

Preparation of A_2SnI_4 Crystals. Hydriodic acid (57%) was stored with a trace amount of hypophosphorous acid and distilled before use. Ethanol was thoroughly dehydrated. Freshly distilled hydriodic acid or anhydrous ethanol was added to stoichiometric quantities of purified SnI_2 and the iodide salt of the organic cation under an inert atmosphere. The solids were completely dissolved at $65 \text{ }^\circ\text{C}$ in the case of ethanol or at $75 \text{ }^\circ\text{C}$ in the case of aqueous HI. When the solution was cooled to $5 \text{ }^\circ\text{C}$ at a rate of $1.5 \text{ }^\circ\text{C h}^{-1}$, red to dark-purple platelet crystals were obtained. Preparation of A_2SnI_4 single crystals, followed by characterization of their structural and transport properties, was carried out using the organic cations shown in Figure 1. All the physical measurements were performed using freshly prepared crystals.

Crystal Structure Determination and Band Structure Calculations. X-ray diffraction data were recorded using a Rigaku R-Axis rapid imaging plate diffractometer with graphite-monochromated $Mo \text{ K}\alpha$ radiation ($\lambda = 0.71069 \text{ \AA}$). The crystal structures were solved by direct methods and refined using the TeXsan program package (hydrogen atoms were not included). The crystals were mounted on a glass capillary either directly (for low-temperature measurements) or using an epoxy resin coating. Details of the crystal data and structures can be found in the Supporting Information (Table S1, Figures S1–S7, and the CIF file).

Band structure calculations employing the extended Hückel method were carried out with the CAESER software suite,¹⁴ using the atomic parameters for Sn and I determined by the X-ray structure analyses. The band dispersions of $(C4)_2SnI_4$, $(PEA)_2SnI_4$, $(TRA)_2SnI_4$, $(IC4)_2SnI_4$, $(GABA)_2SnI_4$, and $(AEPi)_2SnI_4$ are included in the Supporting Information (Figures S1 and S3–S7).

Charge-Transport Measurements. DC conductivity measurements were performed using a standard four-probe method. A carbon paste (Dotite) was used to mount two gold wires ($\varphi = 20 \text{ }\mu\text{m}$; current source) at opposite ends of a plate crystal such that the cross section of the crystal was covered with paste and to attach the remaining two (voltage probe) contacts on the surface of the plate. The original thinner (toluene) of the paste was partially evaporated, and tetraline (1,2,3,4-tetrahydronaphthalene) was added. The time spent processing the sample in air was never more than 20 min. The sample chamber in the cryostat was evacuated immediately after the probes were attached, and the sample was kept under vacuum for the duration of the measurements at temperatures between 5 and 300 K. The conductivity value was practically independent of variations in the sample processing time. Prolonged exposure to air was found to increase both contact resistance and sample resistivity.

Thermoelectric power measurements (see Figure S8 of the Supporting Information) were carried out using the same conducting paste and instrument setup.

Results and Discussion

As previously reported,¹ single crystals can be obtained from solutions of both hydriodic acid and polar organic solvents. Two different solvents, concentrated aqueous HI and ethanol, were used in the crystal preparation. Structural and transport measurements gave essentially the same results regardless of the solvent used to grow the crystals. This shows that although HI is chemically reactive, it has no effect on the electronic properties of the material, probably because HI is a reducing agent.

The crystal structures of $(C5di)SnI_4$ and $(IPy)_2SnI_4$ (Figure 2) are representative of the series. Both are typical A_2MX_4 -type layered perovskites, but there are significant differences in their inorganic frameworks. First, the Sn–I bond lengths in the inorganic plane containing the tin atoms and equatorial iodine atoms are different: in $(C5di)SnI_4$, the four bond lengths are nearly equal (ranging from 3.14 to 3.19 \AA), while in $(IPy)_2SnI_4$, two of the bonds are shorter (approximately 2.9 \AA) and the other two are significantly longer (3.47 and 3.66 \AA). Therefore, the SnI_6 octahedrons in $(IPy)_2SnI_4$ are severely deformed in the equatorial plane. The bond lengths between the tin atoms and the axial iodine atoms are similar in the two compounds. Second, the distortion pattern of the perovskite sheet formed by corner-shared SnI_6 octahedrons is different: significant deviation from linearity in the Sn–I–Sn linkage is apparent in $(C5di)SnI_4$, causing buckling of the inorganic plane, whereas the plane is much flatter in $(IPy)_2SnI_4$. Both the Sn–I bond lengths and the Sn–I–Sn bond angles have been reported to affect the electronic band structure.¹⁵ The band structures calculated using the atomic coordinates of the tin and iodine atoms in the two compounds are indeed considerably different (Figure 2, bottom panels).

When electrical contacts between the crystal and the electrodes were made using commercially available conducting pastes or by vacuum evaporation of Au films on the crystal surfaces, the contact resistance exceeded 1 M Ω , and meaningful conductivity measurements were impossible. The high contact resistance can be attributed to the occurrence

(14) Ren, J.; Liang, W.; Whangbo, M.-H. *Crystal and Electronic Structure Analysis Using CAESER*; PrimeColor Software, Inc.: Cary, NC, 1998.

(15) Knutson, J. L.; Martin, J. D.; Mitzi, D. B. *Inorg. Chem.* **2005**, *44*, 4699.

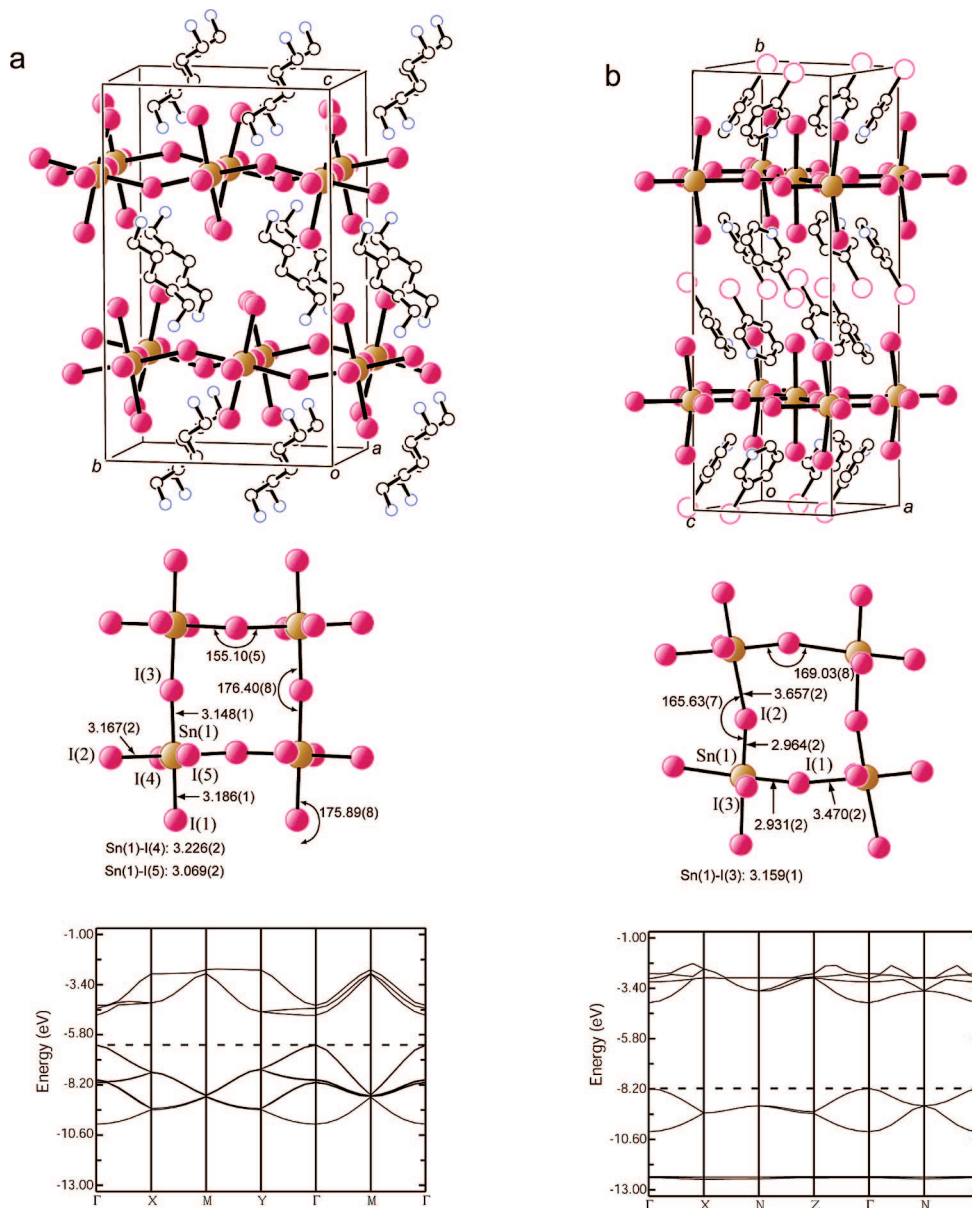


Figure 2. Crystal structure (top), geometry of the inorganic layer (middle), and calculated band structure (bottom) of (a) (C5di)SnI₄ and (b) (IPy)₂SnI₄. Iodine atoms are represented by dark pink spheres and tin atoms by brown spheres. The middle panels show Sn-I bond lengths (Å) and Sn-I-Sn bond angles (deg).

of chemical reactions at the interface. The crystals have high chemical reactivities: they are very sensitive to oxidation and highly soluble in polar organic solvents. Therefore, the conducting material in the paste must be as inert as possible, and we selected carbon. A second requirement is that the solvent used as a paste thinner must not dissolve the crystals. The solvent we selected was tetraline, which is a reducing agent and less polar than the solvents used in commercial pastes. The contact resistance between the crystal and the electrodes was approximately 1000 Ω when a carbon paste thinned by tetraline was used. Although this value is too high for the contact to be considered ideal, it was low enough for four-probe conductivity measurements to be performed. We successfully carried out charge-transport measurements on a series of A₂SnI₄ single crystals using this technique.

The temperature dependence of the resistivity across the perovskite layers is shown in Figure 3. Previously published data¹¹ for a pressed pellet of (C₄)₂SnI₄ are also replotted in

this figure. It is notable that the resistivity of the (C₄)₂SnI₄ single crystal was more than 3 orders of magnitude smaller than that of the powder specimen. Since the resistivity of the pressed pellet is influenced by the contact resistance between grain boundaries and the resistivity along undesirable directions of this anisotropic material, it is clear that single-crystal measurements are required for precise characterization. In addition, the structural transition that takes place at approximately 230 K in (C₄)₂SnI₄ (see Figures S1 and S2 of the Supporting Information) was clearly detected in the temperature dependence of the single-crystal resistivity.

The resistivity is strongly dependent on the type of organic species. The temperature dependence of the resistivity for the A₂SnI₄ crystals having the highest resistance (A = IPy and A₂ = AEPi) corresponds to normal, thermally activated semiconducting behavior. In contrast, the resistivity of the crystals having the lowest resistance (A = TRA, PEA, and C5di) decreases on cooling in the high-temperature region.

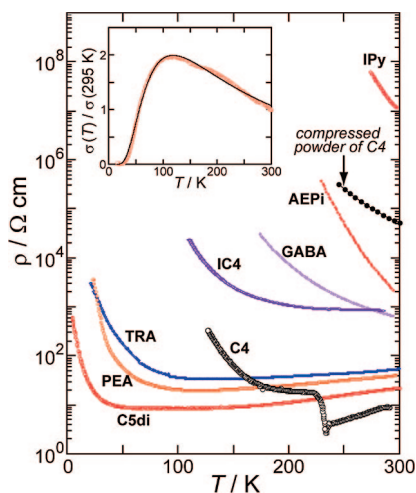


Figure 3. Electrical resistivities (ρ) of A_2SnI_4 compounds as a function of temperature. The cation abbreviations are defined in Figure 1. The compressed powder data for $(C_4)_2SnI_4$ were taken from the literature.¹¹ Inset: Temperature dependence of the normalized conductivity of $(PEA)_2SnI_4$. The solid line is a fit using eq 1 in the text, for which $\alpha = 1.92$ and $E_a = 0.020$ eV.

Table 1. Values of Room-Temperature Resistivity (ρ_{RT}), Activation Energy of Conduction (E_a), Band Gap (E_G), and Width of the Valence Band (W) for A_2SnI_4 Compounds

cation	ρ_{RT} (Ω cm)	E_a (eV) ^a	E_G (eV) ^b	W (eV) ^b
C4	10	phase transition	1.43 ^c	4.01 ^c
C5di	20	0.007	1.43	3.77
PEA	40	0.020	1.48	4.01
TRA	50	0.025	1.56	4.01
IC4	900	0.12	1.72	3.44
GABA	600	0.16	1.62	3.01
AEPi	2000	0.50	2.95	2.63
IPy	10^7	0.52	4.09	2.06

^a From fitting eq 1. ^b From band structure calculations. ^c Value for the room-temperature form.

In all cases, thermally activated behavior was observed at low temperature. The resistivity data could thus be fitted over the entire temperature range by the following equation:

$$\sigma(T)/\sigma(295 \text{ K}) = AT^{-\alpha} \exp(-E_a/kT) \quad (1)$$

where σ is the conductivity (inverse resistivity), k is the Boltzmann constant, and the parameters A , α , and E_a (the activation energy of conduction) are variables whose values are extracted from the fitting procedure. This equation is applicable to narrow-gap systems that show apparent metallic behavior at high temperature,¹⁶ where the temperature dependence of the resistivity is expressed as the product of carrier mobility ($\mu \propto T^{-\alpha}$) and carrier concentration [$n_c \propto \exp(-E_a/kT)$]. The fitted curve for $(PEA)_2SnI_4$ is shown in the inset to Figure 3 as an example. The values of E_a extracted from the fitting procedure are summarized in Table 1, together with the room-temperature resistivities. These results show that when the resistivity is low, E_a tends to be smaller than about 0.02 eV. However, the band structure in Figure 2 shows that the band gap (E_G) in $(C5di)SnI_4$ is larger than 1 eV. The values of E_G obtained from the band structure calculations are also shown in Table 1 and are always more than 1 order of magnitude larger than E_a .

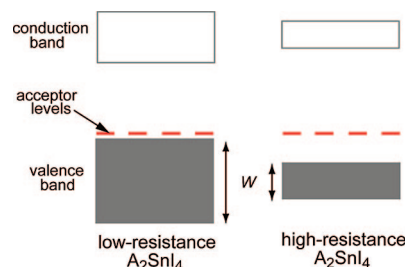


Figure 4. Schematic representations of the electronic structures of low- and high-resistance A_2SnI_4 compounds.

As mentioned above, the structure of the tin iodide perovskite layer in the low-resistance compound $(C5di)SnI_4$ is considerably different from that in the high-resistance compound $(IPy)_2SnI_4$. This difference is prominently reflected in the calculated widths (W in Table 1) of the valence band, which is nearly twice as wide in $(C5di)SnI_4$ as in $(IPy)_2SnI_4$. As W decreases, E_G inevitably becomes larger.

Since E_G is significantly different from E_a , it is clear that there are energy levels in the band gap. The large positive values observed in the thermoelectric power measurements (approximately $400 \mu\text{V deg}^{-1}$ at room temperature for the low-resistance A_2SnI_4 crystals—see Figure S8 of the Supporting Information) indicate that the major charge carriers are holes. Consequently, the mechanism of hole conduction is facilitated by the excitation of electrons from the valence band to acceptor levels in the band gap. The acceptor levels are thought to be formed 0.01–0.02 eV above the top of the valence band when W is large and much further above the valence band when W is small, as shown schematically in Figure 4. When W is small, the hole mobility should also be small. Therefore, the high resistivity of the compounds with small W is thought to be due to small hole mobility and large activation energy.

The next task is to determine how these acceptor levels can be formed. The main components of the valence band are occupied Sn 5s and I 5p orbitals. Therefore, the vacant acceptor levels close to the top of the valence band may be formed by oxidation of the SnI_4^{2-} unit. That is, although the stoichiometry is nominally $(A^+)_2(SnI_4^{2-})$, the actual anion in the perovskite layers in the as-grown crystals may be $SnI_4^{(2-x)-}$. The mobility (μ) at room temperature in low-resistance A_2SnI_4 is expected to be comparable to or slightly less than the value of $50 \text{ cm}^2 \text{ V}^{-1} \text{ s}^{-1}$ measured for a pressed powder sample of the $(CH_3NH_3)SnI_3$ cubic perovskite¹⁰ and much higher than the value of $0.6 \text{ cm}^2 \text{ V}^{-1} \text{ s}^{-1}$ measured for a spin-coated film of $(PEA)_2SnI_4$.¹⁷ Therefore, the concentration of acceptor sites (n_A) can be estimated from the relationship $\sigma = n_A e \mu \exp(-E_a/kT)$, where e is the electron charge. Assuming that $\mu = 10 \text{ cm}^2 \text{ V}^{-1} \text{ s}^{-1}$, the value of n_A is found to be less than 0.01% of the total number of tin sites.

The concept described above regarding the formation of acceptor levels prompted us to attempt artificial p-type doping. Oxidation of SnI_4^{2-} to $SnI_4^{(2-x)-}$ may be considered the same as incorporation of Sn^{IV} or I^0 into the inorganic

(16) Epstein, A. J.; Conwell, E. M.; Miller, J. S. *Ann. N.Y. Acad. Sci.* **1978**, *313*, 183.

(17) Kagen, C. R.; Mitzi, D. B.; Dimitrakopoulos, C. D. *Science* **1999**, *286*, 945.

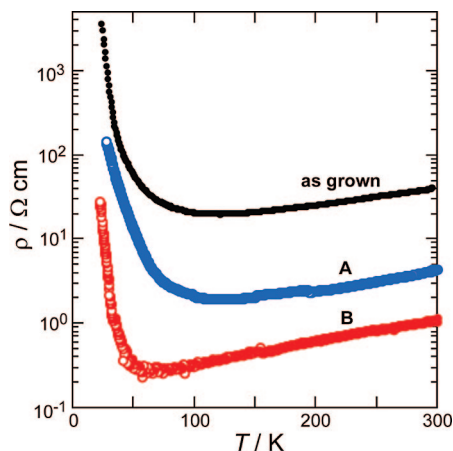


Figure 5. Electrical resistivities of doped $(\text{PEA})_2\text{SnI}_4$ crystals. Crystals A and B were obtained from solutions in which 10% and 20%, respectively, of the total tin content was Sn^{IV} .

layer. We prepared $(\text{PEA})_2\text{SnI}_4$ crystals using an ethanol solution containing SnI_4 . Two types of crystals were prepared: replacing 10% of the SnI_2 in the original solution with SnI_4 gave SnI_4 -doped crystal A, and replacing 20% of the SnI_2 gave SnI_4 -doped crystal B. The appearance of both crystals was essentially the same as that of the original, as-grown crystal. The temperature dependence of the resistivities of these SnI_4 -doped crystals is shown in Figure 5.

The room-temperature resistivity of A was 1 order of magnitude less than that of the as-grown crystal, and the resistivity of B was even smaller. Since the room-temperature resistivity of $(\text{PEA})_2\text{SnI}_4$ prepared without SnI_4 was always found to be in the range 30–100 Ω cm for several batches under different crystal-growth conditions, the lower resistivity values of A and B (1–4 Ω cm) indicate that artificial p-type doping was achieved to some extent in these crystals. At low temperature, the resistivities of both A and B again showed an upturn, indicating thermally activated behavior. When the resistivity of B was fitted to eq 1, a value of 0.015 eV was obtained for E_a . The concentration of acceptor sites estimated using this value is still less than 1%. Therefore, although the Sn^{IV} content in the crystal-growth solution was 20% for B, only a small portion of the Sn^{IV} was found to be incorporated into the crystal. We expect that the maximum

possible extent of doping is subject to limitations imposed by the equilibrium conditions for crystal growth.

If chemical species originating from SnI_4 are incorporated into the crystal, there would also be defects at the cationic sites (due to partial deprotonation of the cations) in order to maintain charge neutrality. We have not managed to detect such defects in the doped crystals using X-ray diffraction because the concentration of defects is still too low. However, if the degree of doping is dictated by cation deficiency, it might be possible to increase the extent of doping by controlling the number of defects at the cation sites.

Conclusion

The high electrical conductivity of A_2SnI_4 -type organic–inorganic hybrids has been verified using improved charge-transport measurements. Since these hybrids have well-defined energy gaps that are larger than 1 eV, the highly conducting nature is attributed to spontaneous hole doping in the as-grown state. Further enhancement of the conductivity can be achieved by artificial hole doping. The inorganic framework that is responsible for the charge transport can be modified by the type of organic cationic species used. Charge transport in the A_2SnI_4 hybrids can thus be tuned by both the organic species and the doping concentration. As found by Mitzi et al.,¹¹ electrical conductivity in a series of $\text{A}_2(\text{CH}_3\text{NH}_3)_{n-1}\text{Sn}_n\text{I}_{3n+1}$ compounds can be further modified by the number of perovskite layers: with increasing n , the conductivity increased. Since increasing n simply reduces E_G successively,³ high conductivity with $n > 1$ may also be related to the spontaneous doping. These materials are soluble in eco-friendly ethanol and show technological promise as semiconductors with tunable electronic properties.

Acknowledgment. This work was supported in part by Grants-in-Aid for Scientific Research from the Ministry of Education, Culture, Sports, Science and Technology, Government of Japan.

Supporting Information Available: A table of crystal data for A_2SnI_4 and figures showing the crystal structure, geometry of the inorganic layer, calculated band structure, and thermoelectric power of A_2SnI_4 (PDF). An X-ray crystallographic file (CIF). This material is available free of charge via the Internet at <http://pubs.acs.org>.

CM702405C